

Tethering a Human with a Quadruped Robot: A Guide Dog to Help Visually Impaired People

Viviana Morlando, Vincenzo Lippiello, Fabio Ruggiero

Abstract—This paper devises a framework to control a quadruped robot tethered to a visually impaired person. The whole-body control of the quadruped robot does not exploit any force sensor. It makes use of two observers: the former for the estimation of the wrench applied on the robot’s centre of mass, which is in turn used to handle the human-robot estimation; the latter for the estimation of the external forces acting on the legs to guarantee a stable balance on irregular terrains. Besides, an admittance filter is employed to guarantee a safe human-robot interaction. A supervisor is designed and placed side by side with the quadruped whole-body control to understand human needs and handle lifelike situations. The validity of the approach is tested in a realistic simulation environment.

I. INTRODUCTION

Over the years, different strategies were realized to assist walking impaired people, like exoskeletons [1], [2] or robot wheelchairs [3], [4]. In this paper, the focus is on people suffering from a visual disease. To this end, different robotic systems were developed, usually employing wheeled robots. One of the first examples was presented in [5], where the robot has an internal map of the environment, can detect obstacles using onboard sensors, and communicates to the blind individual the clear path to follow. Another guiding device employing a wheeled robot is the GuideCane [6]. It is equipped with sonar sensors to detect obstacles, while the computer inside the cane reads the information and constructs a rudimentary map of the environment. Then, it computes a path to guide the cane around obstacles [7]. Different devices inspired by the GuideCane were also developed [8]. Other solutions employ a robotic shopping trolley [9], [10] guiding the person through its handle.

In the cases mentioned above, the connection between humans and robots always happens through a rigid link, limiting the human-robot interaction’s flexibility and ability to operate in narrow spaces. For this reason, recent works started to explore the possibility of using a leash to connect the robot with the person [11], [12], [13], [14]. The leash can be considered a hybrid system, switching from a taut to a slack condition. The human-robot system’s dimensions change whenever the leash becomes slack, allowing the

The research leading to these results has been supported by the PRINBOT project, in the frame of the PRIN 2017 research program, grant number 20172HHNK5.002, the COWBOT project, in the frame of the PRIN 2020 research program, grant number 2020NH7EAZ.002, and the AERIAL-CORE project (Horizon 2020 Grant Agreement No. 871479).

The authors are with the PRISMA Lab, Department of Electrical Engineering and Information Technology, University of Naples Federico II, Via Claudio 21, Naples, 80125, Italy. Authors e-mail: viviana.morlando@unina.it, vincenzo.lippiello@unina.it, fabio.ruggiero@unina.it.

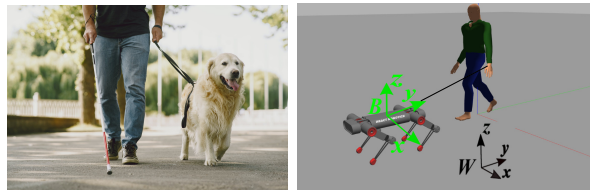


Fig. 1. On the left, a guide dog helping a visually impaired person. On the right, a quadruped is connected to a human through a leash in the Gazebo simulation environment.

robot to guide the human through narrow spaces [11]. A leash-guided interaction is used in [12], in which a physical connection tightly couples a human and an aerial robot. In this case, the human holds a handle which is in turn connected to an aerial vehicle through a cable.

The robots considered in the literature above have evident problems guiding visually impaired people. Wheeled robots have problems adapting to irregularities of the terrain. They are unfeasible in anthropic environments, usually designed for not disabled people with stairs, holes, and obstacles. The propellers’ noise of aerial robots interferes instead with human hearing, which is a vital resource for visually impaired people. Indeed, it is often used to understand the dangers around them: for example, before crossing a road, the guide dog stops and waits for the human to give it the order to cross the street after having heard that there are no cars. For these reasons, this paper focuses on legged robots, especially quadrupeds, playing the role of guide dogs. A quadruped robot can quickly adapt to terrain irregularities and go up and down stairs, and it usually produces less noise than aerial vehicles. The paper’s intention is far from replacing a natural guide dog (see Fig. 1), which also gives the visually impaired person emotional aid. However, a robotic guide dog may have some advantages: it can require less training, it can be easily re-programmed based on the user’s need, and it can be connected to the human’s biological data to call emergency numbers immediately in case of problems.

To the best of the authors’ knowledge, the first attempt to create a tethered system exploiting a quadruped robot as a guide dog is carried out in [11]. The authors presented a method that introduces a quadrupedal robot with a leash to enable the robot-guiding-human system to change its intrinsic dimension to fit in narrow spaces. However, in all the approaches based on a leash-guided system, measuring the force applied between the leash and the robot is necessary. This need is usually satisfied using a force sensor [11], [12], [13], [14]. Besides, a component that can understand human signals is often missing.

In this paper, a framework for using a tethered robot quadruped as a guide dog is devised, exploiting an observer to retrieve the information about the leash force. Such an observer is based on the system momentum for the angular part of the estimated wrench, while it is based on the system acceleration for the translational one. Another observer, based on the system's momentum, is instead used to deal with terrain irregularities acting directly on the quadruped's legs. An admittance filter is also employed to guarantee a safe human-robot interaction. Besides, a supervisor is designed and placed side by side with the quadruped whole-body control to understand human needs and handle realistic situations. The validity of the approach is tested in a physics-engine-based simulation environment as Gazebo (see Fig. 1).

The paper's contribution is twofold, namely, (i) the realization of a framework for a guide-dog quadruped robot, employing two observers: the former for the estimation of the force applied on the robot's centre of mass (CoM) that is in turn used to handle the human-robot estimation, the latter for the estimation of the external forces acting on the legs to guarantee a stable balance on irregular terrains; (ii) the realization of a supervisor based on the interaction force measured through the observer.

II. DYNAMIC MODEL AND OBSERVER

A. Model formulation

Legged robots are usually modelled as a free-floating base with some legs attached. Let \mathcal{B} be the frame whose position is attached to the robot's CoM and whose orientation is the one of a fixed frame on the main body, and let \mathcal{W} be the fixed world frame (Fig. 1). The free-floating base is modelled through 6 virtual joints giving 6 degrees of freedom (DoFs) with respect to \mathcal{W} . Moreover, $n_l \geq 2$ legs are attached to the floating base, giving other nn_l DoFs to the structure, with $n > 0$ joints for each leg. Let $x_{com} = [x_c \ y_c \ z_c]^T \in \mathbb{R}^3$, $\dot{x}_{com} \in \mathbb{R}^3$, and $\ddot{x}_{com} \in \mathbb{R}^3$ be the position, velocity, and acceleration of the frame \mathcal{B} 's origin with respect to \mathcal{W} , respectively. Besides, let $\omega_{com} \in \mathbb{R}^3$ and $\dot{\omega}_{com} \in \mathbb{R}^3$ be the angular velocity and the angular acceleration of \mathcal{B} with respect to \mathcal{W} , respectively. The orientation of \mathcal{B} with respect to \mathcal{W} is expressed by the rotation matrix $R_b \in SO(3)$, from which it can be extracted the set of ZYX Euler angles $\phi \in \mathbb{R}^3$. Finally, $q \in \mathbb{R}^{nn_l}$ is the vector collecting the legs' joints. The dynamic model of a legged robot can be formulated in terms of the global CoM through the transformation introduced in [15]. With this transformation, and assuming that the main's body angular motion is slow, a decoupled structure for the dynamic model is obtained [16], [17], [18]. The inertia matrix is $M(q) = \begin{bmatrix} M_{com,l}(q) & O_{3 \times 3} & O_{3 \times nn_l} \\ O_{3 \times 3} & M_{com,a}(q) & O_{3 \times nn_l} \\ O_{nn_l \times 3} & O_{nn_l \times 3} & M_q(q) \end{bmatrix} \in \mathbb{R}^{(6+nn_l) \times (6+nn_l)}$; the vector accounting for Coriolis, centripetal, and gravitational forces is $h(q, v) = \begin{bmatrix} O_{6 \times (6+nn_l)} \\ C_q(q, v) \end{bmatrix} v + \begin{bmatrix} mg \\ 0_{nn_l} \end{bmatrix}$, with $C_q(q, v) \in \mathbb{R}^{nn_l \times (6+nn_l)}$, where $v =$

$[\dot{x}_{com}^T \ \omega_{com}^T \ \dot{q}^T]^T \in \mathbb{R}^{6+nn_l}$ is the stacked velocity; $m > 0$ is the total mass of the robot, $g = [g_0^T \ 0_3^T]^T \in \mathbb{R}^6$, and $g_0 \in \mathbb{R}^3$ the gravity vector; 0_x and O_x the zero vector and matrix of proper dimensions. The resultant model is

$$M(q)\dot{v} + h(q, v) = S^T \tau + J_{st}(q)^T f_{gr} + J(q)^T f_e + S_w^T w_{e,c}, \quad (1)$$

with $S = [O_{nn_l \times 6} \ I_{nn_l}]$ the selection matrix of the actuated part; $\tau \in \mathbb{R}^{nn_l}$ the joint actuation torques; $f_{gr} \in \mathbb{R}^{3n_{st}}$ the ground reaction forces, with $0 < n_{st} \leq n_l$ the number of stance legs; $f_e \in \mathbb{R}^{3n_l}$ the stacked vector containing the resultant external force at the legs' tips; $S_w = [I_{6 \times 6} \ O_{6 \times nn_l}]$ the selection matrix of the unactuated part; $w_{e,c} = [f_{e,c}^T \ \tau_{e,c}^T]^T \in \mathbb{R}^6$ the external wrench acting directly on the CoM (the external torques resulting at the legs' tip are negligible considering a robot with point feet); $J_{st}(q) = [J_{st,com}(q) \ J_{st,j}(q)] \in \mathbb{R}^{3n_{st} \times 6+nn_l}$ and $J(q) = [J_{com}(q) \ J_j(q)] \in \mathbb{R}^{3n_l \times 6+nn_l}$ Jacobian matrices that are defined in [16]. It can be noticed that the CoM's dynamics are included in the first six rows of (1), decoupled from the legs' dynamics included in the other nn_l rows. The resultant external forces at the legs' tip, f_e , can be considered as contacts that dictates a net wrench on the CoM, while the wrench directly applied to the CoM, $w_{e,c}$, influences only the CoM's dynamics and it constitutes in this work the leash tension with some other minor external disturbances.

B. Observers

Given the decoupled structure of the legged robot's dynamics (1), two observers are designed as in [19], in which the wrench on the CoM and the forces on the legs are estimated separately. In detail, the observer for the CoM is composed of a momentum-based observer for the angular term and an acceleration-based observer for the translational one, employing directly measurable values from the on-board sensors. This composition will be referred to as *hybrid* in this paper. The observer for the legs is the momentum-based observer presented in [16].

1) *Estimation for the CoM*: Consider the angular centroidal's dynamics composed of the second set of three rows in (1). The generalized angular momentum is expressed as

$$\rho = M_{com,a}\omega. \quad (2)$$

Considering the above-mentioned assumption that the main's body angular motion is slow, the expression $\frac{d}{dt}(M_{com,a}\omega) = M_{com,a}\dot{\omega}$ holds, meaning that the effect of precession and nutation of the rotating body are discarded [18]. Then, taking into account (1), the time derivative of (2) is $\dot{\rho} = J_{st,com,a}^T f_{gr} + J_{com,a}^T f_e + \tau_{e,c}$, with $J_{st,com,a} \in \mathbb{R}^{3n_{st} \times 3}$ and $J_{com,a} \in \mathbb{R}^{3n_l \times 3}$ the Jacobians whose transpose map the ground reaction and the external forces into the angular acceleration of the CoM, respectively. Without loss of generality, from (1), define $\tau_c = J_{com,a}^T f_e + \tau_{e,c} \in \mathbb{R}^3$ as the total external torques acting at the CoM, and $\hat{\tau}_c$ as its estimation. The straightforward objective is to achieve $\hat{\tau}_c \simeq \tau_c$. The

estimator is designed in the time domain as

$$\hat{\tau}_c(t) = K_a \left(\rho(t) - \int_0^t (\hat{\tau}_c(\sigma) + J_{st,com,a}^T f_{gr}) d\sigma \right), \quad (3)$$

where $K_a \in \mathbb{R}^{3 \times 3}$ is a positive definite gain matrix. Moreover, it is assumed that $\rho(0) = 0$, meaning that the estimator's kick off should be prior to the robot control. In this case only the angular velocity, available from the inertia and measurement unit (IMU), is required. The estimator's dynamics can be written as $\dot{\hat{\tau}}_c + K_a \hat{\tau}_c = K_a \tau_e$, that represents a linear exponentially stable system.

To compute the translational component of the wrench acting on the CoM, an acceleration-based observer can be used employing the measurements of the IMU on the floating base. Considering the linear centroidal's dynamics composed of the first set of three rows in (1), it can be obtained

$$J_{com,l}^T f_e + f_{e,c} = M_{com,l} \ddot{x}_{com} + mg - J_{st,com,l}^T f_{gr}, \quad (4)$$

with $J_{st,com,l} \in \mathbb{R}^{3n_{st} \times 3}$ and $J_{com,l} \in \mathbb{R}^{3n_l \times 3}$ the Jacobians whose transpose map the ground reaction and the external forces into the linear acceleration of the CoM, respectively. From (1), consider $f_c = J_{com,l}^T f_e + f_{e,c} \in \mathbb{R}^3$ as the current total external force at the CoM, and $\hat{f}_c \in \mathbb{R}^3$ as the estimated one. The following first-order stable filter can be applied

$$\dot{\hat{f}}_c(t) = K_l \int_0^t (M_{com,l} \ddot{x}_{com} + mg - J_{st,com,l}^T f_{gr} - \hat{f}_c) d\sigma \quad (5)$$

to obtain the estimator's dynamics $\dot{\hat{f}}_c + K_l \hat{f}_c = K_l f_c$, where $K_l \in \mathbb{R}^{3 \times 3}$ is a positive definite gain matrix.

2) *Estimation for the legs:* For the disturbances acting on the legs, the last nn_l rows of (1) are considered. Consider $f_j = J_j^T f_e \in \mathbb{R}^{nn_l}$ as the effect at the joint torques of the resultant force at the legs' tips, and $\hat{f}_j \in \mathbb{R}^{nn_l}$ as its estimation, respectively. The chosen second-order observer can be written as $\dot{\hat{f}}_j(t) = K_{2,j} \int_0^t (-\hat{f}_j(\sigma) + K_{1,j} (\rho_j(t) + \int_0^t (\hat{f}_j(\sigma) + C_q^T \dot{q} + \tau + J_{st,j}^T f_{gr}) d\sigma)) d\sigma$, with $K_{1,j}, K_{2,j} \in \mathbb{R}^{(nn_l) \times (nn_l)}$ positive definite gain matrices. Further details related to this observer can be found in [16]. Recalling the external forces at the legs' tips f_e , its estimation $\hat{f}_e \in \mathbb{R}^{3n_l}$ can be retrieved through

$$\hat{f}_e = J_j^{T\dagger} \hat{f}_j \quad (6)$$

To recap, the hybrid observer is composed of (3) and (5) and it estimates the interaction with the human through the leash, while the observer on the legs is given by (6). It should be noticed that the information about ground reaction forces f_{gr} is obtained by embedded sensors on robot's feet.

C. Human-robot system

The relation between the human and the robot can be defined as a function of the two connection points of the leash: $p_h \in \mathbb{R}^3$ for the human's hand, and $x_r \in \mathbb{R}^3$ for the robot, considering it as the CoM of the trunk of the robot which is a fixed point, $p_h = x_r - l\bar{v}_l$, where $l > 0$ is the distance between the robot and the human, and $\bar{v}_l \in \mathbb{R}^3$ is the unit vector pointing from the human

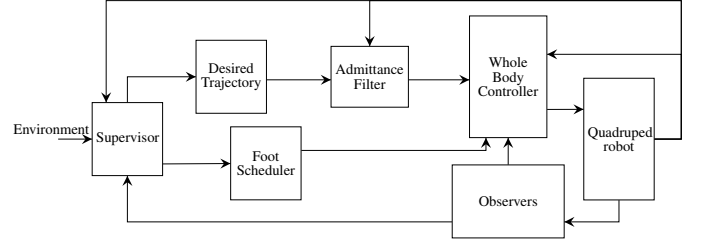


Fig. 2. Conceptual block scheme of the devised framework.

to the robot along the leash. It is important to consider the interaction between the human and the robot. As reported in [12], such kind of tasks can be performed considering the human's dynamics as a mass-spring-damper system. Let $m_h \in \mathbb{R}_{>0}$ be the human's mass; $C_h \in \mathbb{R}_{>0}^{3 \times 3}$ be the system's damping; $g_h = m_h g_0 \in \mathbb{R}^3$; $f_{h,ext} \in \mathbb{R}^3$ be the vector containing external forces acting on the human and $v_h \in \mathbb{R}^3$ be the human's linear velocity. The human's dynamics can be written as $m_h \dot{v}_h + C_h v_h + g_h = f_{h,ext} - f_{e,c}$. Given the assumption in Section II-A about the slowness of the main's body angular motion, it can be considered that most of the leash wrench is contained in the translational force, representing the most critical information about the human-robot interaction. For this reason, the leash can be modeled as a spring with stiffness $k > 0$ through the Hooke's law, so that the leash force is

$$\|f_{e,c}\| = \begin{cases} k(l - \bar{l}) & \text{if } (l - \bar{l}) > 0 \\ 0 & \text{if } (l - \bar{l}) \leq 0 \end{cases} \quad (7)$$

where \bar{l} represents the nominal length of the leash. Whenever the leash is taut, $(l - \bar{l}) > 0$, and a force is applied between the robot and the human, so that the human is guided by the robot.

III. DEVISED FRAMEWORK

The framework is composed of a motion planner, a foot scheduler, an admittance filter, a whole-body controller, the observers described above and a supervisor. The block scheme can be observed in Fig. 2.

A. Motion planning

The motion is continuously re-planned so that the zero moment point is always maintained inside the support polygon [20]. From now on, the position and the orientation of the frame \mathcal{B} are stacked into $r_c = [x_{com}^T \ \phi^T]^T \in \mathbb{R}^6$, while its velocity and acceleration can be considered $v = [\dot{x}_{com}^T \ \dot{\omega}_{com}^T]^T \in \mathbb{R}^6$ and $\dot{v}_c = [\ddot{x}_{com}^T \ \ddot{\omega}_{com}^T]^T \in \mathbb{R}^6$. The motion planner computes the references $r_{c,ref}$, $\dot{r}_{c,ref}$ and $\ddot{r}_{c,ref} \in \mathbb{R}^6$ for the CoM and the reference $x_{sw,des}$, $\dot{x}_{sw,des}$ and $\ddot{x}_{sw,des} \in \mathbb{R}^{3(n_l - n_{st})}$ for the swing feet as a 3-rd order splines. Further details can be found in [16].

B. Admittance filter

The idea of an admittance control scheme is to modify the reference position of the robot $x_{com,ref} \in \mathbb{R}^3$ based on the leash force. It should be observed that this control is

performed only for the translational part, given the above assumption that the essential information about the human-robot interaction is given through the linear force.

The admittance controller guarantees a safe human-robot interaction so that the robot's motion adapts to the human one. In this way, the robot can accelerate or decelerate based on the cable's tension, avoiding overcoming human capabilities. To obtain the modified reference trajectory, $x_{com,mod} \in \mathbb{R}^3$, the desired admittance model can be considered as

$$M_a \ddot{\tilde{x}} + D_a \dot{\tilde{x}} + K_a \tilde{x} = f_d - \hat{f}_c, \quad (8)$$

where $\tilde{r} = x_{com,mod} - x_{com,ref}$, and M_a , D_a , and $K_a \in \mathbb{R}^{3 \times 3}$ are the desired inertia, damper, and stiffness matrices of the desired admittance model, respectively. In order to achieve a desired human-robot behaviour, $f_d \in \mathbb{R}^3$ is the desired leash force empirically chosen to maximize the velocity of the robot without pulling too much the human.

C. Whole-Body Controller

The wrench-based optimization problem used in this paper is based on [16] with suitable modifications to include the hybrid estimator. Let $\zeta = [\dot{r}_c^T \quad \dot{q}^T \quad f_{gr}^T]^T \in \mathbb{R}^{6+nn_l+3n_{st}}$ be the chosen control variables. The addressed problem is

$$\underset{\zeta}{\text{minimize}} \quad f(\zeta) \quad (9)$$

$$\text{subject to} \quad A\zeta = b, \quad (10)$$

$$D\zeta \leq c. \quad (11)$$

The detail for each term of the is detailed in the following.

1) *Cost function*: The cost function tracks the CoM's reference coming from the motion planner, reducing as much as possible the control effort. To this aim, the desired wrench at the robot's CoM is computed using the first six equations of (1) and the references from the motion planner, as $w_{com,des} = K_p(r_{c,ref} - r_c) + K_d(\dot{r}_{c,ref} - \dot{r}_c) + mg + M_{com}(q)\ddot{r}_{c,ref}$, with $K_p, K_d \in \mathbb{R}^{6 \times 6}$ positive definite matrices. Let $\hat{w}_{com} = [\hat{f}_c^T \quad \hat{\tau}_c^T]^T$ be the estimated external wrench at the CoM, the cost function minimizing the desired wrench and compensating for the leash tension can be written as $f(\zeta) = \|J_{st,com}^T \Sigma \zeta - (w_{com,des} - \hat{w}_{com})\|_Q + \|\zeta\|_R$, with $\Sigma \in \mathbb{R}^{3n_{st} \times (6+nn_l+3n_{st})}$ a matrix selecting the last $3n_{st}$ elements of ζ , $Q \in \mathbb{R}^{6 \times 6}$ and $R \in \mathbb{R}^{(6+nn_l+3n_{st}) \times (6+nn_l+3n_{st})}$ two symmetric and positive definite matrices that can be used to specify the relative weight between the components of the cost function, and $\|\cdot\|_x$ the quadratic form with proper matrix.

2) *Equality constraints*: Two equality constraints need to be imposed. The first one regards the dynamic consistency, employing the first six rows of (1) as $[M_{com}(q) \quad 0_{6 \times nn_l} \quad -J_{st,com}(q)^T] \zeta = -mg$. The second equality constraint maintains the contact of the stance feet imposing their velocity equal to zero as $J_{st}(q)v = 0_{3n_{st}}$, whose time derivative is $[J_{st,com} \quad J_{st,j} \quad O_{3n_{st} \times 3n_{st}}] \zeta = -\dot{J}_{st,com}\dot{r}_c - \dot{J}_{st,j}\dot{q}$.

3) *Inequality constraints*: To avoid slipping, ground reaction forces need to be constrained inside a friction cone, approximated as a pyramid to obtain linear constraints in the problem. Considering the i -th ground reaction force $f_{gr,i} \in \mathbb{R}^3$, with $i = 1, \dots, n_{st}$, and indicating with $\bar{n}_i \in \mathbb{R}^3$ the i -th normal versor, $\bar{l}_{1,i}, \bar{l}_{2,i} \in \mathbb{R}^3$ two tangential versor related to the i -th contact with the ground, $\mu > 0$ the friction coefficient, the constraints can be written as [21]

$$\begin{aligned} (\bar{l}_{1,i} - \mu \bar{n}_i)^T f_{gr,i} &\leq 0, & -(\bar{l}_{1,i} + \mu \bar{n}_i)^T f_{gr,i} &\leq 0, \\ (\bar{l}_{2,i} - \mu \bar{n}_i)^T f_{gr,i} &\leq 0, & -(\bar{l}_{2,i} + \mu \bar{n}_i)^T f_{gr,i} &\leq 0. \end{aligned} \quad (12)$$

For mechanical and safety reasons, constraints to limit the joint torques need to be imposed $\tau_{min} - C_q(q, v)\dot{q} \leq [O_{nn_l \times 6} \quad M_q(q) \quad -J_{st,j}(q)^T] \zeta \leq \tau_{max} - C_q(q, v)\dot{q}$, where $\tau_{min}, \tau_{max} \in \mathbb{R}^{nn_l}$ are the minimum and maximum torques and the last nn_l rows of (1) were considered.

The last constraint allows the robot to follow the trajectory planned for the swing feet. This constraint exploits the estimation of external forces from (6) acting on swing legs $\hat{f}_{e,sw} \in \mathbb{R}^{3(n_l - n_{st})}$. These disturbances can heavily affect the respective foot's motion, causing a drift. To compensate for them, operational space formulation for swing feet is employed, using the following command acceleration $\ddot{x}_{sw,c} = \ddot{x}_{sw,d} + K_{d,sw}(\dot{x}_{sw,d} - \dot{x}_{sw}) + K_{p,sw}(x_{sw,d} - x_{sw}) - J_{sw}M_c^{-1}P J_{sw}^T \hat{f}_{e,sw}$, with $M_c = PM + I_{6+nn_l} - P$ and $P \in \mathbb{R}^{6+nn_l \times 6+nn_l}$ an orthogonal projection operator [16]. This constraint is softened by adding slack variables $\gamma \in \mathbb{R}^{3(n_l - n_{st})}$. The addressed inequality constraint is $\ddot{x}_{sw,c} - \gamma - \dot{J}_{sw}v \leq [J_{sw,com} \quad J_{sw,j} \quad O_{3(n_l - n_{st}) \times 3n_{st}}] \zeta \leq \ddot{x}_{sw,c} + \gamma - \dot{J}_{sw}v$ [16].

4) *Control torques*: Given the result of the optimization problem, the control torques can be computed using the last nn_l rows of (1) as $\tau = M_q(q)\dot{q} + C_q(q, v)\dot{q} - J_{st,j}(q)^T f_{gr}$, considering that all the external forces have been compensated for inside the quadratic problem.

D. Supervisor

A supervisor is employed to decide how the robot should act based on the intention of the human or the environment. Such a supervisor is inspired by the training of guide dogs in reality. Whenever the dog meets an obstacle or a dangerous situation, it usually: (i) stops its motions; (ii) waits for the human to understand the situation; (iii) waits for an input to continue the path and, eventually, some information about the new trajectory to follow [22], [23]. Usually, visually impaired people are trained to understand the situation by using a cane or hearing. They are also trained to understand what is better to do afterwards, telling the dog the new command. In the following, the robot is supposed to be endowed with sensors and algorithms allowing it to detect obstacles or dangerous situations: the implementation of these skills are out of the scope of this paper.

The devised supervisor should not only start and stop the movement of the robot based on the leash tension, but it should also change the robot forward direction based on the estimated cable's force \hat{f}_c . The supervisor's behaviour can be resumed in Algorithm 1. It is based on the following

Algorithm 1 SUPERVISOR

```
1: if  $\|\hat{f}_c\| > \bar{\sigma}$  and MOVE then
2:   STOP
3: else if  $\|\hat{f}_c\| > \bar{\sigma}$  and STOP then
4:   MOVE and new direction
5: else if env and MOVE then
6:   STOP
7: else
8:   keep doing what is doing
9: end if
```

states and commands: *MOVE*, the state indicating that the robot is moving; *STOP*, the state indicating that the robot is not moving; *new direction*, the new direction the dog must follow and that is computed based on the estimated force $\hat{f}_c = [\hat{f}_{c,x} \ \hat{f}_{c,y} \ \hat{f}_{c,z}]^T$, meaning that the desired yaw angle for the robot is computed as $\varphi = \text{Atan2}(\hat{f}_{c,x}, \hat{f}_{c,y})$, where Atan2 is the arctangent function of two arguments [24]; $\bar{\sigma} > 0$, a threshold for the leash force indicating the pulling of the leash by the human; *env*, a Boolean variable indicating the detection of obstacles or dangerous situations.

IV. CASE STUDIES

A. Setup

Simulations have been carried out through the ROS middleware and the physics-engine-based simulator Gazebo. Using a Gazebo plugin, the human is simulated by approximating the model to a mass-spring-damper system. Another plugin simulates the leash's force through the equation (7). The quadruped used for simulations is the DogBot from React Robotics, an open-source platform whose structure is shown in Fig. 1. Details about the quadruped's structure can be found in [16]. All the simulations were performed on a standard personal computer. The torque control loop, the state estimation, and the momentum-based observation have a frequency of 1 kHz, while the optimization problem runs at a frequency of 400 Hz. In the following, it is experimentally chosen $\bar{\sigma} = 50$ N. For further information related to the controller parameter, the gains of the observer and the leash stiffness, the code is available¹. The related video² shows the addressed case studies and additional ones.

B. Case study 1

This case study tests the framework's capabilities on a rectilinear trajectory, characterized by a change in the velocity profile of the human and a sudden stop, testing the robot's capabilities to adapt its motion to the human. The robot is forced to follow a rectilinear trajectory along the y -axis of \mathcal{W} . The desired force f_d presented in the admittance filter in (8) has been empirically chosen in the forward direction y as $f_{d,y} = 30$ N. This force keeps the cable in tension, applying reasonable force on the human. As shown in Fig. 3, the actual applied force remains bounded around

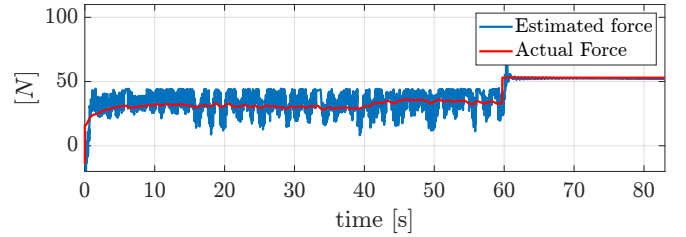


Fig. 3. Case study 1. Estimated force (blue) and actual force (red).

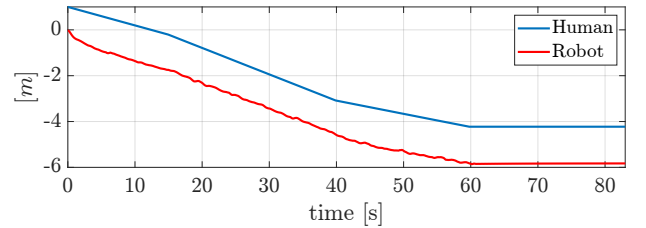


Fig. 4. Case study 1. Human (blue) and robot (red) positions.

this chosen value, overcoming the threshold at the instant $t = 62$ seconds when the human suddenly stops. It can also be observed that the reconstructed force has some oscillations and uncertainties, probably given by parametric uncertainties and the approximations made to obtain the decoupled model in Section II-A. However, it can be seen in the accompanying video that this estimation helps the robot retain balance and maintain a good gait also in the presence of the leash tension. In order to show the capability of the framework to adapt the robot's velocity to the human one, the same case on a rectilinear trajectory has been tested considering a human's velocity with a sinusoidal trend. The velocities for both the human and the robot can be appreciated in Fig. 6. The human's velocity change can be appreciated in Fig. 4, observing the slope of his position. The distance l between the human and the robot can be observed in Fig. 5, as introduced in (7). Notice that it remains constant, validating the performance of the admittance controller that adapts the robot's velocity to the human, guaranteeing a safe motion.

C. Case study 2

This case study aims to demonstrate the framework capabilities along a curved trajectory. In order to guide the human, the robot can not immediately change its orientation while standing at the same point. Otherwise, the human will not understand where it is going, and the leash could also be slack without giving the human any information regarding the direction. For this reason, the robot should perform a curved trajectory to change its direction, constantly imposing a force on the leash that, even if it changes the orientation, can guide the human through a similar curved trajectory. The resultant trajectories performed by both the human and the robot can be seen in Fig. 8, noticing that the human can finally smoothly change his direction. Also in this case, the resultant leash force is bounded thanks to the admittance controller (see Fig. 7) with its estimation.

D. Case study 3

Suppose the dog meets an obstacle on the path ($env = 1$). In this case, it usually stops its walking, waits for the human

¹<https://github.com/prisma-lab/Tethering-human-with-quadruped>

²<https://youtu.be/ON4t58CdDzQ>

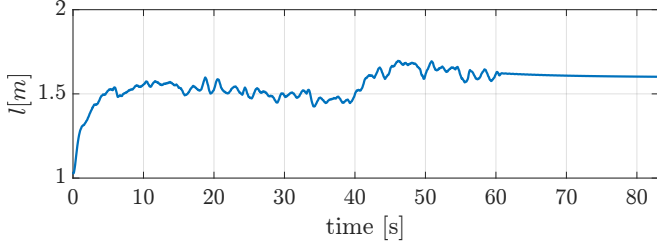


Fig. 5. Case study 1. Distance l between the robot and the human.

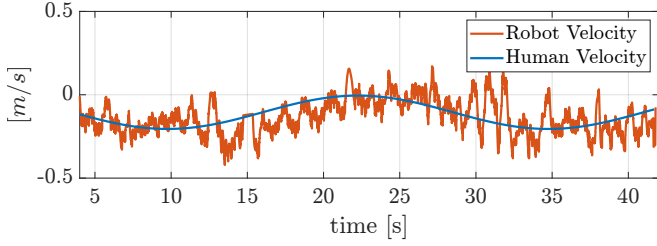


Fig. 6. Case study 1. Human (blue) and robot (red) velocities in the sinusoidal trend.

to understand the situation or a signal to continue, and some information about the new trajectory to follow. This case study aims to test the observer to understand when the robot should restart. However, it uses this estimation to retrieve the direction of the new trajectory decided by the human (i.e., the impressed leash force). In this case, a simple scenario with only one obstacle is considered (see Fig. 9). In Fig. 10, the estimations for both x -axis and y -axis can be observed. It can be noticed that for the first part of the path, most of the leash force is along the y -axis since this is the direction of the path. From instant $t = 16$ to $t = 36$ seconds, the estimated force is lower regarding the movement phase, so the leash can be considered almost slack, and the human understands that the dog has stopped. Afterwards, the human understands which is the best direction to follow, rotates to align with it, and gives the robot a pull along the x -axis to start moving in that direction. Indeed, at instant $t = 36$ seconds, the estimated force $\hat{f}_{c,x}$ along the x -axis is greater than 50 N, which is the threshold for the leash force. For the rest of the path, most of the leash force is along the x -axis because the robot is now moving in this direction.

V. CONCLUSION AND FUTURE WORK

A framework for a guide-dog quadruped robot was presented in this paper. The devised architecture employs two observers to obtain information about the leash force, reject external disturbances, and retain the balance on irregular terrains. A supervisor based on the interaction force measured through the observer is included and is employed to decide how the robot should act based on the human's intentions or the environment. The validity of the approach is demonstrated through simulations in Gazebo. The performances of the devised observers can be improved through artificial intelligence and deep learning techniques, expanding the range of human-robot interactions. Practical validation of the framework is also foreseen.

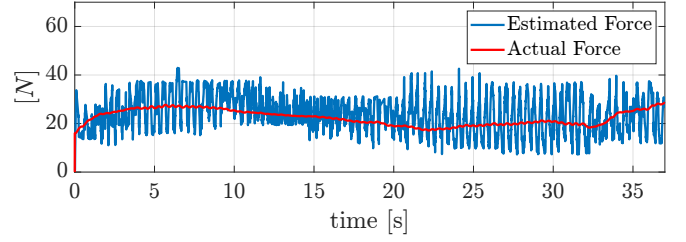


Fig. 7. Case study 2. Estimated force (blue) and actual force (red).

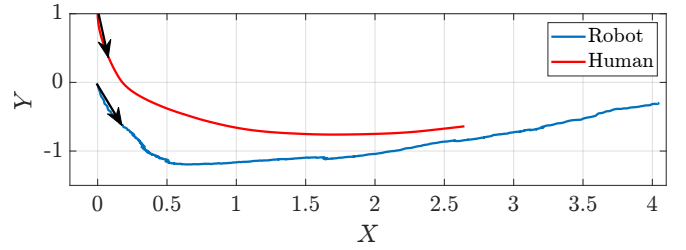


Fig. 8. Case study 2. Human (red) and robot (blue) trajectories. The arrows indicate the starting points.

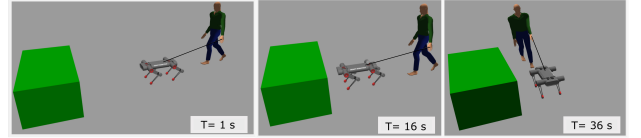
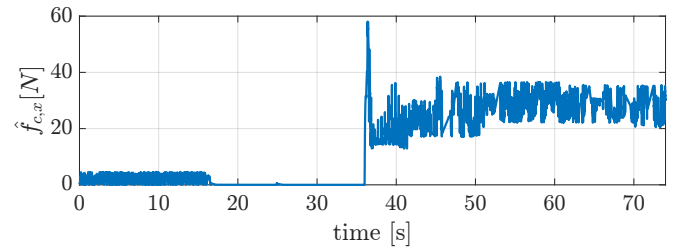
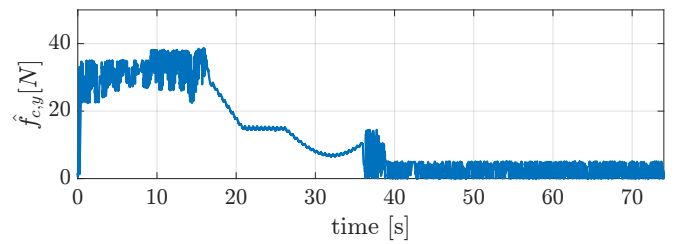


Fig. 9. Case Study 3. Scenario and movements.



(a)



(b)

Fig. 10. Case Study 3. Estimated force along the x - (a) and the y - (b) axes.

REFERENCES

- [1] Z. Shen, Y. Zhuang, J. Zhou, J. Gao, and R. Song, "Design and test of admittance control with inner adaptive robust position control for a lower limb rehabilitation robot," *International Journal of Control, Automation and Systems*, vol. 18, no. 1, pp. 134–142, 2020.
- [2] Q. Wu, X. Wang, B. Chen, and H. Wu, "Development of a minimal-intervention-based admittance control strategy for upper extremity rehabilitation exoskeleton," *IEEE Transactions on Systems, Man, and Cybernetics: Systems*, vol. 48, no. 6, pp. 1005–1016, 2017.
- [3] L. Teng, M. A. Gull, and S. Bai, "Pd-based fuzzy sliding mode control of a wheelchair exoskeleton robot," *IEEE/ASME Transactions on Mechatronics*, vol. 25, no. 5, pp. 2546–2555, 2020.
- [4] H. Ikeda, T. Toyama, D. Maki, K. Sato, and E. Nakano, "Cooperative step-climbing strategy using an autonomous wheelchair and a robot," *Robotics and Autonomous Systems*, vol. 135, p. 103670, 2021.
- [5] S. Tachi, K. Tanie, K. Komoriya, Y. Hosoda, and M. Abe, "Guide dog robot—its basic plan and some experiments with meldog mark i," *Mechanism and Machine Theory*, vol. 16, no. 1, pp. 21–29, 1981.
- [6] J. Borenstein and I. Ulrich, "The guidecane—a computerized travel aid for the active guidance of blind pedestrians," in *Proceedings of International Conference on Robotics and Automation*, vol. 2. IEEE, 1997, pp. 1283–1288.
- [7] M. Bousbia-Salah and M. Fezari, "A navigation tool for blind people," in *Innovations and advanced techniques in computer and information sciences and engineering*. Springer, 2007, pp. 333–337.
- [8] A. A. Melvin, B. Prabu, R. Nagarajan, B. Illias, A. Allan Melvin, B. Prabu, R. Nagarajan, I. Bukhari, and A. Melvin, "Rovi: a robot for visually impaired for collision-free navigation," in *Proc. of the International Conference on Man-Machine Systems (ICoMMS 2009)*, 2009, pp. 3B5–1.
- [9] C. P. Gharpure and V. A. Kulyukin, "Robot-assisted shopping for the blind: issues in spatial cognition and product selection," *Intelligent Service Robotics*, vol. 1, no. 3, pp. 237–251, 2008.
- [10] V. Kulyukin and A. Kutiyawala, "Accessible shopping systems for blind and visually impaired individuals: Design requirements and the state of the art," *The Open Rehabilitation Journal*, vol. 3, no. 1, 2010.
- [11] A. Xiao, W. Tong, L. Yang, J. Zeng, Z. Li, and K. Sreenath, "Robotic guide dog: Leading a human with leash-guided hybrid physical interaction," in *2021 IEEE International Conference on Robotics and Automation (ICRA)*. IEEE, 2021, pp. 11 470–11 476.
- [12] M. Tognon, R. Alami, and B. Siciliano, "Physical human-robot interaction with a tethered aerial vehicle: Application to a force-based human guiding problem," *IEEE Transactions on Robotics*, vol. 37, no. 3, pp. 723–734, 2021.
- [13] K. A. Hamed, V. R. Kamidi, W.-L. Ma, A. Leonessa, and A. D. Ames, "Hierarchical and safe motion control for cooperative locomotion of robotic guide dogs and humans: A hybrid systems approach," *IEEE Robotics and Automation Letters*, vol. 5, no. 1, pp. 56–63, 2019.
- [14] J. E. Young, Y. Kamiyama, J. Reichenbach, T. Igarashi, and E. Sharlin, "How to walk a robot: A dog-leash human-robot interface," in *2011 RO-MAN*. IEEE, 2011, pp. 376–382.
- [15] C. Ott, M. A. Roa, and G. Hirzinger, "Posture and balance control for biped robots based on contact force optimization," in *2011 11th IEEE-RAS International Conference on Humanoid Robots*, 2011, pp. 26–33.
- [16] V. Morlando, A. Teimoorzadeh, and F. Ruggiero, "Whole-body control with disturbance rejection through a momentum-based observer for quadruped robots," *Mechanism and Machine Theory*, vol. 164, p. 104412, 2021.
- [17] B. Henze, C. Ott, and M. Roa, "Posture and balance control for humanoid robots in multi-contact scenarios based on model predictive control," in *2014 IEEE/RSJ International Conference on Intelligent Robots and Systems*, 2014, pp. 3253–3258.
- [18] J. Di Carlo, P. M. Wensing, B. Katz, G. Bledt, and S. Kim, "Dynamic locomotion in the mit cheetah 3 through convex model-predictive control," in *2018 IEEE/RSJ International Conference on Intelligent Robots and Systems*, 2018, pp. 1–9.
- [19] V. Morlando and F. Ruggiero, "Disturbance rejection for legged robots through a hybrid observer," in *2022 30th Mediterranean Conference on Control and Automation (MED)*. IEEE, 2022, pp. 743–748.
- [20] C. D. Bellicoso, F. Jenelten, P. Fankhauser, C. Gehring, J. Hwangbo, and M. Hutter, "Dynamic locomotion and whole-body control for quadrupedal robots," in *2017 IEEE/RSJ International Conference on Intelligent Robots and Systems*, 2017, pp. 3359–3365.
- [21] C. D. Bellicoso, C. Gehring, J. Hwangbo, P. Fankhauser, and M. Hutter, "Perception-less terrain adaptation through whole body control and hierarchical optimization," in *2016 IEEE-RAS 16th International Conference on Humanoid Robots*, 2016, pp. 558–564.
- [22] R. T. Edwards, ""forward!" the experience of a new guide dog owner," *Bmj*, vol. 325, no. 7356, p. 171, 2002.
- [23] B. Due and S. Lange, "Semiotic resources for navigation: A video ethnographic study of blind people's uses of the white cane and a guide dog for navigating in urban areas," *Semiotica*, vol. 2018, no. 222, pp. 287–312, 2018.
- [24] B. Siciliano, L. Sciavicco, L. Villani, and G. Oriolo, *Robotics: modelling, planning and control*. Springer, 2010.